Bioconjugate Chemistry

pubs.acs.org/bc

Article

Design and Functional Analysis of Heterobifunctional Multivalent Phage Capsid Inhibitors Blocking the Entry of Influenza Virus

Lutz Adam, Eva Müller, Kai Ludwig, Simon Klenk, Daniel Lauster, Susanne Liese, Andreas Herrmann,* and Christian P. R. Hackenberger*

Cite This: *Bioconjugate Chem.* 2022, 33, 1269−1278

Read Online

ACCESS | Metrics & More | Article Recommendations | Supporting Information

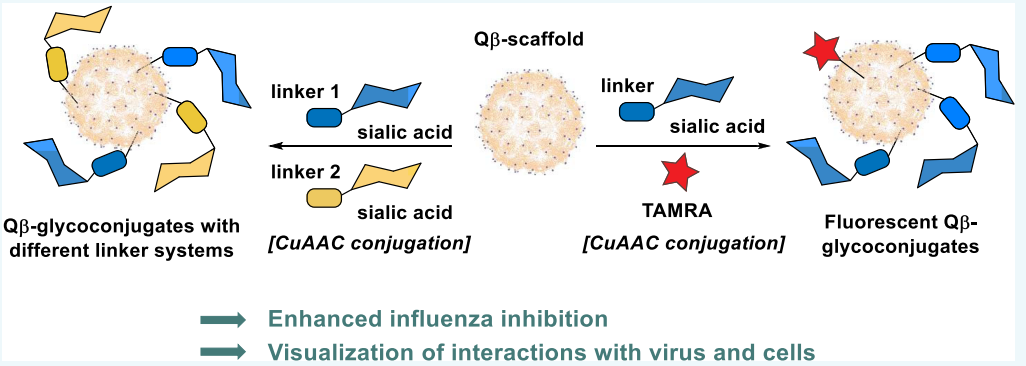

ABSTRACT: Multiple conjugation of virus-binding ligands to multivalent carriers is a prominent strategy to construct highly affine virus binders for the inhibition of viral entry into host cells. In a previous study, we introduced rationally designed sialic acid conjugates of bacteriophages (Qβ) that match the triangular binding site geometry on hemagglutinin spike proteins of influenza A virions, resulting in effective infection inhibition *in vitro* and *in vivo*. In this work, we demonstrate that even partially sialylated Qβ conjugates retain the inhibitory effect despite reduced activity. These observations not only support the importance of trivalent binding events in preserving high affinity, as supported by computational modeling, but also allow us to construct heterobifunctional modalities. Capsids carrying two different sialic acid ligand−linker structures showed higher viral inhibition than their monofunctional counterparts. Furthermore, capsids carrying a fluorescent dye in addition to sialic acid ligands were used to track their interaction with cells. These findings support exploring broader applications as multivalent inhibitors in the future.

INTRODUCTION

Hemagglutinin (HA), the most abundant spike protein of influenza A and B viruses, is a promising target for antivirals to complement currently licensed therapeutics and reduce the risk of emerging drug-resistant strains.[1] Specific binding of an inhibitor to HA can be achieved by mimicking its natural host cell receptor, *i.e.*, terminal sialic acid (SA) residues of the glycocalyx, through the multivalent presentation of *N*-acetylneuraminic acid (Neu5Ac) derivatives or sialyl oligosaccharides. Alternatively, peptides[2] or aptamers[3] have been used to furnish multivalent conjugates with antiviral activity *in vitro* and *in vivo*. Among SA-based HA-binding inhibitors, different concepts regarding special prearrangement of carbohydrates have been explored. While some approaches rely on rather flexible scaffolds, *e.g.*, linear polymers[4−9] or mostly arbitrary structures, such as hyperbranched or dendritic polymers,[4,10] gold nanoparticles,[11] proteins,[12−14] nanogels,[15] virus-like particles,[16] carbon nanostructures,[17,18] phospholipid micelles,[19,20] or lipid bilayers,[21] others employ a rational design to tailor SA positions to match the triangular HA receptor binding site (RBS) geometry. For instance, the architecture of a tripodal inhibitor with a peptide scaffold by Waldmann et al. was inspired by detailed *in silico* analysis of the HA head domain topology.[22] Other systems achieve accurate spacing of carbohydrate ligands using cyclic peptides[23] or PNA−DNA oligomers[24] as structural elements.

Recently, our laboratory has contributed to the rational engineering of influenza inhibitors by introducing structurally defined Qβ-sialoside conjugates as SA-based HA inhibitors.[25] We used an engineered version of the highly symmetrical Qβ-bacteriophage-carrying homopropargylglycine (Hpg) at specific positions in the capsid protein (Qβ[Hpg] (**1**), see Scheme 1) to immobilize azide-containing Neu5Ac derivatives *via* variable

Received: April 4, 2022
Revised: May 25, 2022
Published: June 27, 2022

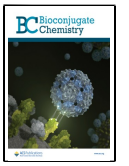

Scheme 1. Reaction Scheme for the Preparation of (A) Fully and (B) Partially Monofunctionalized Qβ Sialosides by CuAAC. (C) One-Pot CuAAC Synthesis of Bifunctional Qβ Sialosides with Different EG-Linker Lengths[a]

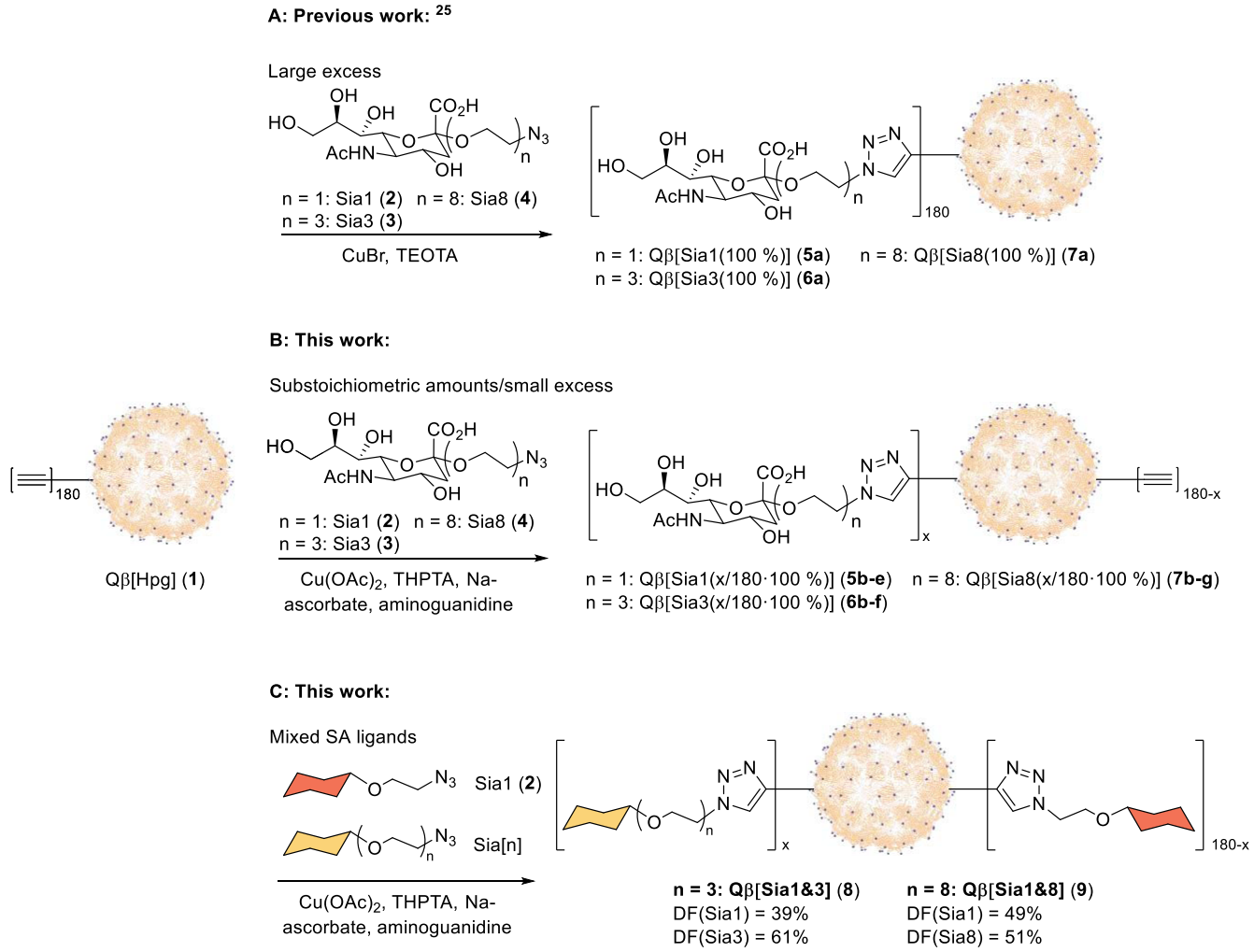

[a]THPTA: Tris(3-hydroxypropyltriazolylmethyl)amine. Protein structure of Qβ-bacteriophage capsid (protein data bank (PDB) #1QBE) published in ref 26.[26]

ethylene glycol (EG) linkers (Sia1 (**2**), Sia3 (**3**), Sia8 (**4**) for n = 1, 3, 8 according to Scheme 1, respectively) using Cu-catalyzed alkyne−azide cycloaddition (CuAAC). Thereby, we precisely matched the triple-symmetric geometrical arrangement of the HA RBS and were able to demonstrate potent neutralization of various influenza strains *in vitro* and *in vivo* by preventing binding to host cells. In our previous study, conjugates with shorter linkers generally showed higher inhibitory potency than those with longer linkers, which can likely be attributed to their lower flexibility and therefore higher fidelity to the prearranged configuration. Data obtained by cryogenic transmission electron microscopy (cryoTEM) and microscale thermophoresis-based affinity studies with HA suggested that individual functionalized capsids tend to interact with single HA trimers, thus supporting the notion of a trivalent binding mode. However, multivalent interactions must be conceived as dynamic complexes composed of individually associating and dissociating receptor−ligand pairs. Consequently, the maximum possible valency is not always equal to the functional valency, which is the valency in the most probable binding state.[26] So far, we had no comprehensive experimental evidence to evaluate the contribution of mono- and bivalent interactions to the overall affinity of Qβ sialosides. The same report applied a statistical mechanics model, which quantitatively predicted a parameter of HA affinity, the equilibrium binding constant K_D, for various Qβ sialosides assuming exclusively trivalent interactions between the capsids and HA. These values showed a strong correlation (nearly identical values) with the binding inhibitory constant K_i (sometimes referred to as the hemagglutination inhibition titer), which is a common measure for the potency of influenza inhibitors and is obtained experimentally by the hemagglutination inhibition (HAI) test (for further information see refs 27−29).

In the current study, we first set out to examine whether the quality of prediction holds up in scenarios where trivalent binding is limited to gain more insight into the binding pattern. To this end, we prepared a library of partially functionalized Qβ sialosides using decreasing amounts of sialic acid azide linkers in CuAAC reactions, which resulted in unoccupied positions in the triangular prearrangement of the SA ligands. Afterward, we compared their inhibitory potencies to the theoretical values. In doing so, we ensured that the probability of mono- and bivalent binding motives increases with decreasing degree of functionalization (DF). This would not be the case for mixtures of fully

https://doi.org/10.1021/acs.bioconjchem.2c00166
Bioconjugate Chem. 2022, 33, 1269−1278

and nonsialylated capsids with the same overall DF, for instance a 1:1 mixture of capsids with DF = 100 and 0% to achieve an overall 50% of occupied conjugation sites.

Building on insights we gained during this study, we furthermore constructed several heterobifunctional influenza inhibitors with different SA linkers or fluorescent labels attached. We used these modalities to study the fate of Qβ sialosides in a cellular environment, which we could not address in the previous publication. Of particular interest was to unravel whether capsids would be taken up by cells *via* nonspecific interactions with the cell surface or in complex with influenza viruses.

RESULTS AND DISCUSSION

Partially functionalized Qβ sialosides were prepared from Qβ[Hpg] (**1**) following a modified version of the CuAAC protocol published previously.[25] Here, we controlled the DF by the amount of SA azide added to the reaction (Scheme 1B and Table 1) (see Materials and Methods). Capsids with linker lengths n = 1, 3, and 8 and DF values ranging from ca. 20 to 100% were subsequently examined for HA binding of influenza A virus (IAV) H3N2 strain X31 (A/X31) in an HAI test (see Materials and Methods). The determined inhibition constant K_i reflects the lowest inhibitor concentration to achieve 100% hemagglutination inhibition.[27−29] In all cases, an exponential increase of K_i was observed with decreasing DF. Remarkably, we found considerable inhibitory potency even at a DF of only 20% for all functionalized capsid variants independent of their EG-linker lengths. However, the increase was less steeper for longer linker variants (Figure 1). It can be hypothesized that this results from the ability of longer linkers to form alternative triangular configurations to compensate for unoccupied sugar positions. Further repeated measurements using capsid variants with linker lengths n = 3 and 8 from the same stock solution lead to equal K_i values from which no standard deviation could be determined (see Supporting Information). This is not uncommon as replicate K_i values from the HAI assay typically only differ by a factor of 2, which becomes more prominent for lower affine compounds (*e.g.*, Sia8 with 20% DF).[29] We surmise, as illustrated in Figure 2, that short and inflexible linkers allow trivalent interactions between capsids and HA only at faces where each conjugation site is occupied by SA. Instead, longer linkers could make it possible to rescue trivalent binding by substituting a vacant SA position with SA from a neighboring face.

Table 1. Obtained DF in Qβ-Sialoside Bioconjugations in Relation to Input Azide per Hpg

SA azide	equivalents/Hpg	obtained DF [%]	product number
Sia1 (**2**)	15	100	**5a**
	1	85	**5b**
	0.75	67	**5c**
	0.5	45	**5d**
	0.25	19	**5e**
Sia3 (**3**)	15	100	**6a**
	5	93	**6b**
	3.3	83	**6c**
	1.7	53	**6d**
	1.3	35	**6e**
	0.7	21	**6f**
Sia8 (**4**)	25	100	**7a**
	5	92	**7b**
	3.3	69	**7c**
	1.7	34	**7d**
	1.3	27	**7e**
	1	23	**7f**
	0.7	15	**7g**
Sia1 (**2**)/Sia3 (**3**)	7.5/7.5	39/61	**8**
Sia1 (**2**)/Sia8 (**4**)	7.5/7.5	49/51	**9**
Sia1 (**2**)/TAMRA-N_3 (**8**)	15/0.075	97/3 (±2%)	**11a**
	15/0.15	90/7 (3% residual Hpg)	**11b**

To follow up on this assumption of binding behavior as a function of linker length, we aimed to obtain the relation between the inhibitory constant K_i and the degree of functionalization theoretically and to compare them with the experimental data to gain insight into the phage binding mode. We noted that, for a fixed linker length, the probability to bind to a SA triplet scales as

$$\exp\left(-\frac{9}{2}\frac{d^2}{r_0^2 n}\right)$$

while the probability to bind to two neighboring SA scales as

$$\exp\left(-3\frac{\bar{d}^2}{r_0^2 n}\right)$$

with d and $\bar{d}$ being the distance that has to be bridged by the linker in the trivalent and divalent binding modes, respectively, n being the polymerization index of the EG linker, and r_0 = 5 Å.[30] Based on these binding probabilities, we define the effective number of matching SA triplets and SA doublets as

$$N_{\mathrm{tri,\,eff}} = \sum_j \exp\left(-\frac{9}{2}\frac{d_j^2}{r_0^2 n}\right),\quad N_{\mathrm{di,\,eff}} = \sum_j \exp\left(-3\frac{\bar{d}_j^2}{r_0^2 n}\right) \tag{1}$$

where we sum over all possible SA triplets and SA doublets of a capsid, weighted with the appropriate binding probability. To determine $N_{\mathrm{tri,eff}}$ and $N_{\mathrm{di,eff}}$ numerically, we generated random configurations of partially functionalized capsids and averaged over 500 configurations. In Figure 1D,E, $N_{\mathrm{tri,eff}}$ and $N_{\mathrm{di,eff}}$ are shown relative to the fully functionalized capsid in dependence of DF. Figure 1D shows a scaling of $N_{\mathrm{tri,eff}} \sim \mathrm{DF}^3$ for short linkers with n = 1, while longer linkers transition to $N_{\mathrm{tri,eff}} \sim \mathrm{DF}^2$. In qualitative terms, the number of possibilities for trivalent binding decreases more strongly for short linkers (n = 1) compared to longer linkers (n = 3 or 8). This behavior is consistent with the possibility of longer linkers to make use of irregular triangular configurations. For the divalent case, we find $N_{\mathrm{di,eff}} \sim \mathrm{DF}^2$ independent of the linker length (Figure 1E). For short linkers (n = 1), tri- and divalent binding show a clearly distinct scaling behavior. In contrast, the number of effective binding possibilities for longer linkers (n = 3 and 8) is approximately proportional to DF^2 for both tri- and divalent binding.

To relate these findings to the inhibitory constants K_i shown in Figure 1A−C, we note that K_i in trivalent and divalent binding modes is inversely proportional to $N_{\mathrm{tri,eff}}$ and $N_{\mathrm{di,eff}}$, respectively. Hence, if the binding mode of capsids with a short linker (n = 1) is dominated by trivalent binding, the inhibitory constant should scale as $K_i \sim \mathrm{DF}^{-3}$, which is confirmed by Figure 1A. The scaling behavior here clearly shows that divalent bonds contribute only

https://doi.org/10.1021/acs.bioconjchem.2c00166
Bioconjugate Chem. 2022, 33, 1269−1278

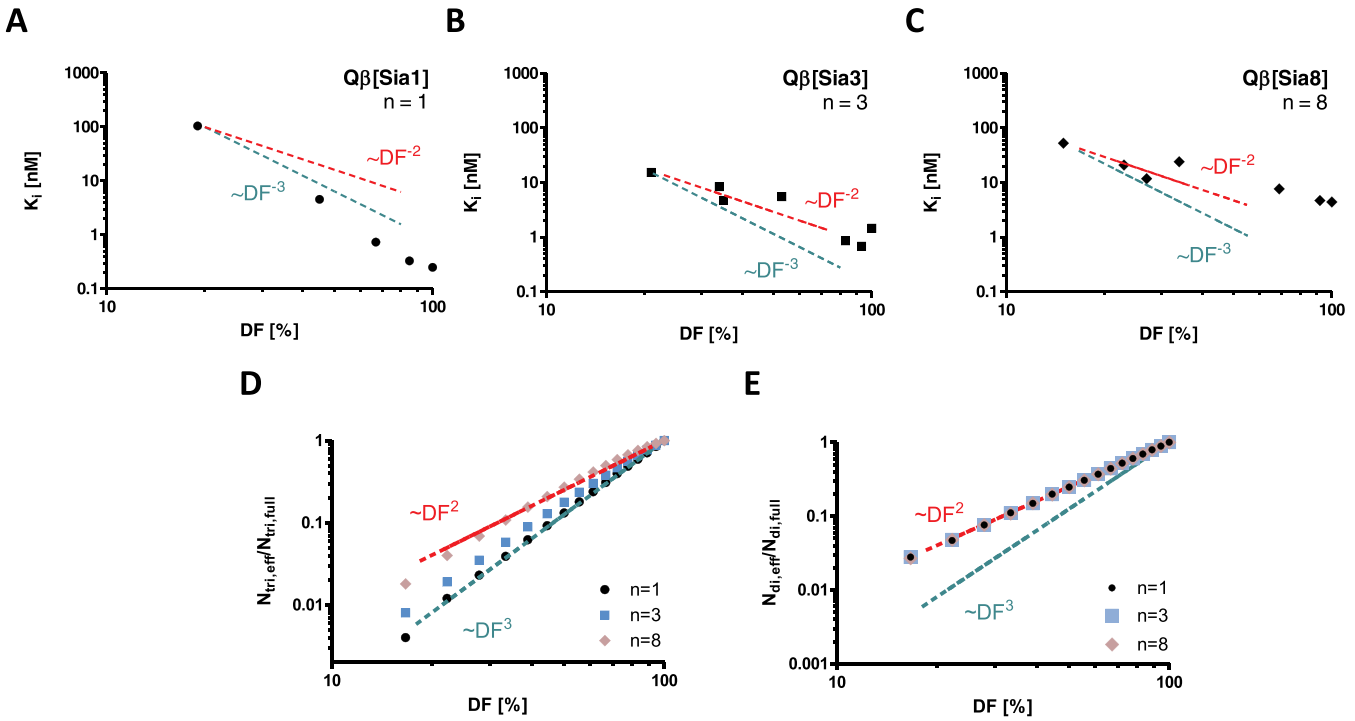

Figure 1. (A–C) Comparison of experimental K_i values of HAI test against influenza A virus (IAV) strain A/X31 (markers) and their theoretically predicted progressions for Qβ sialosides of different linker lengths in relation to DF. n represents the number of EG units in the SA linker. Dashed lines represent theoretical K_i progressions for quadratic (red) and cubic (green) proportionalities between K_i and DF. For n = 1, the slope of the experimental values is in good agreement with a cubic relation between K_i and DF, whereas for n = 3 and 8, the decline is more in line with a quadratic dependency. Data points represent mean values from either two (n = 3 and 8, green and blue) or three (n = 1, black) replicate experiments. Numerical values for experimentally obtained K_i are given in the Supporting Information. (D, E) Effective number of matching SA triplets (D) and SA doublets (E) in relation to DF. All values are given relative to the fully functionalized capsid. The ratio of triplet motives available for virus binding declines in an approximately cubic relation to DF for n = 1 and quadratically for n = 8, while n = 3 shows an intermediate behavior. In contrast, the ratio of available doublet motives scales in a quadratic relation to DF for all linker lengths.

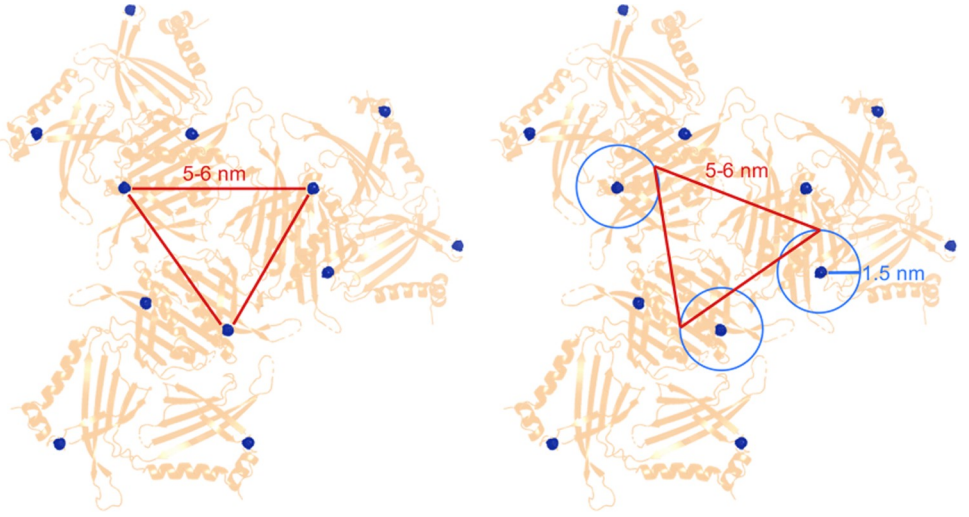

Figure 2. Triangular arrangements of SA azides on the capsid surface. Blue spheres indicate Hpg side chain positions. Red triangles indicate HA RBS geometry. Left: arrangement with minimal distance to Hpg side chains, requiring no linker flexibility. Right: alternative triangular arrangement for a more flexible linker, which substitutes one SA from the minimal distance arrangement with that of a neighboring position. A 1.5 nm (light blue circles) approximately is the most probable end-to-end distance of an EG(8) linker.[25] Protein structure of Qβ-bacteriophage capsid (PDB #1QBE) published in ref 31.[31]

negligibly. The interpretation of the scaling behavior for longer linkers (n = 3 and 8) is more complex, since the slopes found in Figure 1B,C scale roughly with $K_i \sim DF^{-2}$, which is in agreement with both divalent and trivalent binding. We therefore restate a result from our previous study, finding that trivalent binding is the dominant binding mode in fully functionalized capsids.[25] Now, the scaling behavior in Figure 1D,E shows that the ratio between tri- and divalent binding for long linkers $N_{tri,eff}/N_{di,eff} \approx DF^2/DF^2 \approx 1$ can be approximated as independent of DF. The

https://doi.org/10.1021/acs.bioconjchem.2c00166
Bioconjugate Chem. 2022, 33, 1269–1278

dominance of trivalent binding is therefore preserved even for lower DF.

Since all tested variants of sialylated capsids, by interpolation of the obtained data, retained K_i values in the range of 1−10 nM down to 50% sialylation, we hypothesized that it should be possible to employ a portion of the Hpg conjugation sites for the attachment of alternative ligands or fluorescent labels without drastically compromising the inhibitory activity. In our previous study, we found that the inhibition potential of phages toward human pathogenic IAV strains with different HA types depends not only on the SA receptor (SA *vs* 2,3-sialyllactose *vs* 2,6-sialyllactose) but also on the linker length. We concluded that the distance of the SA RBS is slightly different among different HA types.[25] Therefore, we were interested in combining different SA-based ligands on the same capsid to engineer broad-spectrum IAV inhibitors.

In a convenient one-pot protocol, we simply combined two distinct SA azides at equal ratios in our CuAAC conjugations to aim for DF of ∼50% for each ligand. Mixed conjugates of the previously shown Sia[*n*] derivatives (Q*β*[Sia1&3] (**8**) and Q*β*[Sia1&8] (**9**)) were prepared in this fashion (Scheme 1C) and analyzed by mass spectrometry to determine the relative loadings of individual sugars (see the Supporting Information). Inhibition of influenza strain A/X31 by these mixed conjugates was again demonstrated in a HAI test (Figure 3). Interestingly,

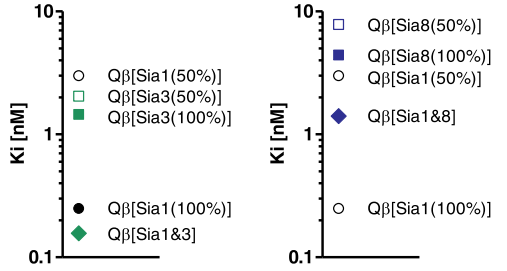

Figure 3. HAI test of mixed linker length Q*β* sialosides against influenza A/X31. K_i values for DF = 50% were interpolated from a regression function of the experimental values shown in Figure 1 (see Materials and Methods). Other data points represent mean values of two (Q*β*[Sia3(100%)], Q*β*[Sia8(100%)], and mixed capsids) or three (Q*β*[Sia1(100%)]) replicate experiments. Numerical values for experimentally obtained K_i are given in the Supporting Information.

Q*β*[Sia1&3] (**8**) showed a higher inhibitory potency (K_i = 0.16 nM) than either of the monofunctional capsids (K_i = 0.25 nM for Q*β*[Sia1(100%)] and K_i = 1.5 nM for Q*β*[Sia3(100%)]), hinting at a possible cooperative effect between these ligands. The K_i value of Q*β*[Sia1&8] (**9**) (K_i = 1.4 nM) is in between those of its monofunctional analogues (K_i = 0.25 nM for Q*β*[Sia1(100%)] and K_i = 4.4 nM for Q*β*[Sia8(100%)]). These first inhibition studies can be regarded as a proof of concept for the feasibility and activity of mixed Q*β* sialosides. As a future perspective, it would be of interest to investigate the inhibitory range of mixed capsids against a wider panel of influenza strains and introduce other ligands such as sialyllactose oligosaccharides or ligands for other influenza surface proteins, which is currently ongoing in our laboratories.

Having established a one-pot protocol to obtain Q*β* capsids with two different labels, we next aimed to synthesize fluorescent Q*β* sialosides to monitor their interactions with viruses and living cells. The fluorescent glycoconjugates were obtained by formally replacing a small amount of the SA in a given Q*β* sialoside with tetramethylrhodamine (TAMRA) as a fluorescent dye. We envisioned that this approach is favorable over unspecific fluorescent labeling reagents, such as succinimide esters targeting other reactive amino acids on the capsid surface, which would yield less well-defined and less reproducible products.

Consequently, we conjugated Sia1 (**2**) and CuAAC-compatible TAMRA azide (**10**) (for synthesis, see the Supporting Information) concomitantly to Q*β*[Hpg] (**1**) by combining them at different ratios in one-pot CuAAC reactions (Scheme 2). A ratio of Sia1 (**2**)/TAMRA azide (**10**) = 199:1 reproducibly afforded conjugates with 3% (±2%) of Hpg side chains modified with the dye and full conversion of the remaining positions with SA (Table 2, entry 1). Higher dye loadings led to incomplete conversion of alkyne functionalities and increasingly hydrophobic products, which aggregated over time and could no longer be analyzed by LC-MS to determine the DF of the sugar and dye (Table 2, entries 2 and 3).

Table 2. SA and Dye Loadings of Bifunctional Q*β* Sialosides as a Result of Different Reagent Ratios in CuAAC

entry	ratio Sia1:TAMRA-N_3	product number	DF (Sia1)	DF (TAMRA)	DF (Hpg)
1	199:1	**11a**	97% (±2%)	3% (±2%)	0%
2	99:1	**11b**	90%	7%	3%
3	49:1 and lower		incomplete conversion: Product too hydrophobic for LC-MS analysis.		

To assess the aggregation propensity of fluorescently labeled capsids, a Q*β*[Sia1(98%),TAMRA(2%)] (**11a**) sample was analyzed using dynamic light scattering (DLS). Freshly prepared, fully sialylated Q*β*[Sia1(100%)] (**5a**) and a visibly aggregated, TAMRA-labeled Q*β* sialoside obtained with a Sia1:TAMRA-N_3 ratio of 4:1 were used as reference samples. Q*β*[Sia1(98%),TAMRA(2%)] (**11a**) showed a uniform population of separate particles directly after preparation and 4%

Scheme 2. Reaction Scheme for One-Pot CuAAC Synthesis of Bifunctional Q*β* Sialosides with TAMRA Fluorescent Label[a]

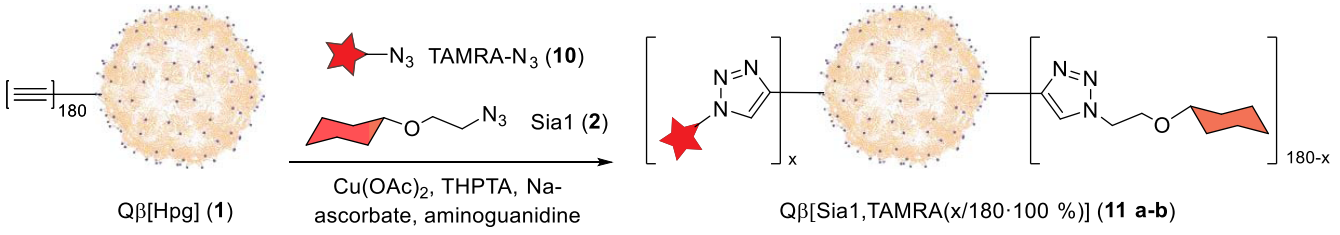

[a]For product DF in relation to reagent ratio, see Table 2.

https://doi.org/10.1021/acs.bioconjchem.2c00166
Bioconjugate Chem. 2022, 33, 1269−1278

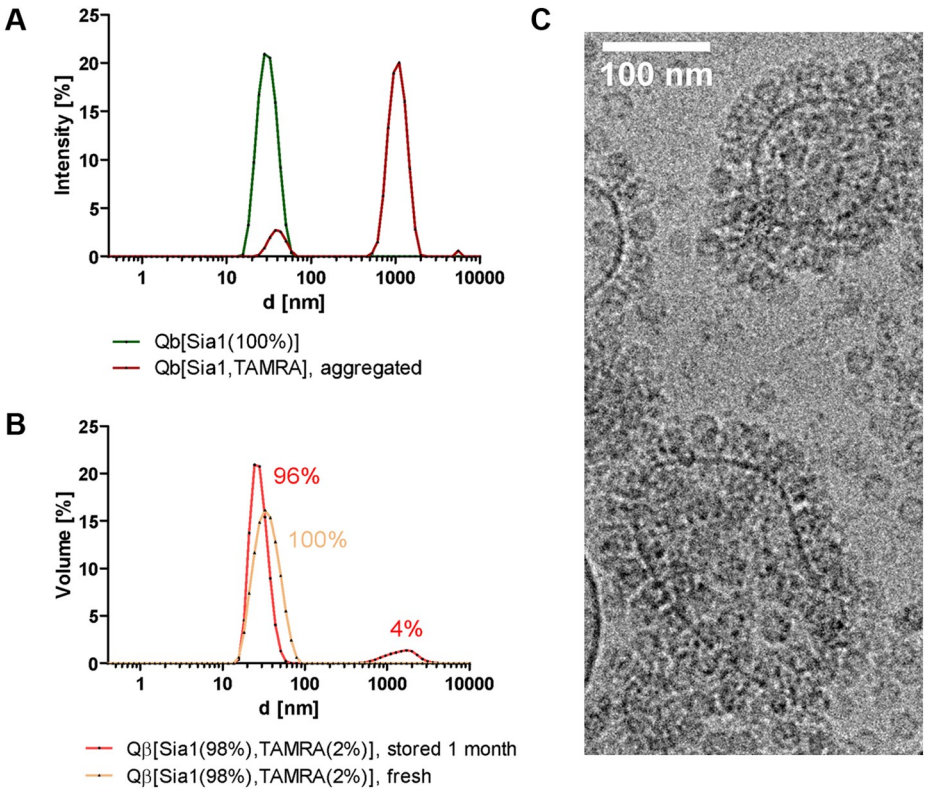

Figure 4. DLS spectra of Qβ sialosides. (A) Light scattering intensity distribution of reference samples. Freshly prepared Qβ[Sia1(100%)] (**5a**) (green curve) shows a uniform population of particles with a diameter of 30 nm, which corresponds in size to the wild-type Qβ bacteriophage.[32] Visibly aggregated Qβ sialosides with high TAMRA loading (red curve) show a second population of aggregates of ca. 1 μm diameter. (B) Qβ[Sia1(98%),TAMRA(2%)] (**11a**) showed 4% aggregation after 1 month of storage at 4 °C. (C) CryoTEM micrograph of Qβ[Sia1(98%),TAMRA(2%)] (**11a**) densely decorating influenza A virions (A/X31).

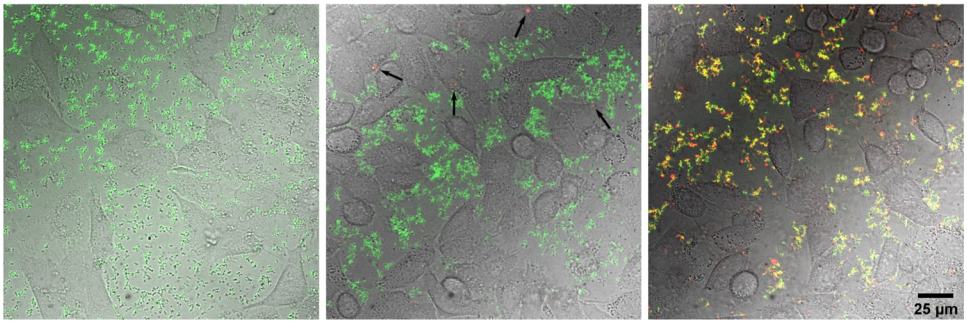

Figure 5. Interaction study of Qβ[Sia1(98%),TAMRA(2%)] (green) with A549 cells. Left: the capsids distribute evenly around healthy cells. No cellular uptake could be observed after incubation of capsids with cells for 20 min at 37 °C. Middle: the capsids show no attachment to A549 cells with bound DiD-labeled viruses A/Panama (red). Cells were preincubated with viruses at 4 °C before addition of capsids. Upon supply of capsids, the cells were incubated for 20 min at 37 °C. Black arrows indicate DiD-labeled influenza virions that have not been internalized into cells. The virus loses its label upon membrane fusion during infection. Right: Virions (A/Panama) and Qβ[Sia1(98%),TAMRA(2%)] (**11a**) form aggregates (yellow) upon preincubation that do not interact with A549 cells.

aggregation after 1 month of storage at 4 °C (Figure 4A,B). Virus binding of fresh Qβ[Sia1(98%),TAMRA(2%)] (**11a**) was furthermore verified by cryoTEM upon incubation with influenza strain A/X31 (Figure 4C).

Next, we examined Qβ[Sia1(98%),TAMRA(2%)] (**11a**) for interaction with A549 cells by fluorescence microscopy (Figure 5). The capsids showed no uptake or apparent interaction, both with healthy and influenza-infected cells. When the virus was preincubated with the inhibitor, we observed the formation of virus−phage aggregates, which also did not interact with cells. For this experiment, we used a more recent seasonal IAV H3N2 strain A/Panama/2007/99 (A/Panama). We have shown recently that Qβ[Sia1] efficiently binds and inhibits host cell entry of this strain comparable to that of A/X31.[25] In future experiments, we plan to use fluorescent Qβ sialosides to study their interactions with other biological environments, such as the respiratory mucus layer. Since mucus can act as a barrier for drug delivery, such studies may yield valuable insights into the ability of Qβ sialosides to penetrate the mucus layer and furthermore provide valuable tool compounds to probe mucus transport in general.

https://doi.org/10.1021/acs.bioconjchem.2c00166
Bioconjugate Chem. 2022, 33, 1269−1278

CONCLUSIONS

In this study, we have shown that a partial reduction of the Sia-DF of Qβ phages keeps the inhibitory effect of influenza virus binding to cells although at a reduced level. The good coincidence of our experimental data with those of a detailed computational modeling strongly suggests that at least a trivalent interaction between functionalized phages and viruses is necessary for binding. Thus, both the DF as well as the linker length are the limiting factors of phage association with the viral spike proteins.

Nevertheless, retention of the inhibitory effect even at reduced DF offers the opportunity to further advance our previously introduced monofunctionalized inhibitors[25] and generate heterofunctional Qβ phages. We took advantage of this by covalently labeling Sia-functionalized phages with a fluorescent dye at very low DF and track interaction of those phages with viruses and host cells. The absence of cellular uptake of phages further strengthens their applicability as extracellularly active antivirals. Even more important, we generated phages carrying two SA with different linker lengths and observed an even higher inhibition potential with respect to monofunctional phages, indicating a cooperative effect by binding to various SA receptors on the phage surface. Thus, these heterofunctional multivalent structures have strong potential for preventing the interaction with host cells for a broader range of viruses. These studies are fundamental for further development not only of the phages used here, but also, in general, for the application of multivalent inhibitors. To prevent rapid emergence of resistance, the use of heterofunctional multivalent inhibitors, *i.e.*, scaffold occupation with ligands that inhibit different targets of the pathogen simultaneously, is an alternative. For example, HA and neuraminidase (NA) can be inhibited simultaneously on the surface of IAV.[16,33]

MATERIALS AND METHODS

Chemicals and Solvents. Chemicals and solvents were obtained from various chemical vendors in reagent grade. All materials were used without further purification unless specified otherwise. SA azides and Qβ[Hpg] (**1**) were obtained as described in the literature.[25]

Virus Strains. Virus strains used were influenza A/X31 (H3N2), which is a laboratory strain reassorted from A/Aichi/2/68 (H3N2) and A/Puerto Rico/8/1934 (H1N1) (in short A/X31), and A/Panama/2007/99 (H3N2) (in short A/Panama).

Analytical LC-MS. LC-MS analysis of Qβ sialosides to determine DF was conducted using an ACQUITY H-class instrument (Waters Corporation) equipped with an ACQUITY UPLC-Protein BEH C4, 300 Å, 1.7 μm, 2.1 mm × 50 mm column (Waters Corporation) and a XEVO G2-XS QTof mass analyzer (Waters Corporation). The liquid phase consisted of mixtures of acetonitrile and water as described above, containing, instead of TFA, 0.01% formic acid (FA) (≥99.0%, Optima LC/MS Grade, Fisher Chemical). The obtained data were processed using the software MassLynx (version 4.1, Waters Corporation) and protein spectra were deconvoluted by the included MaxEnt1 algorithm.

The protein (10 μg) was incubated at 95 °C for 5−10 min and subsequently mixed with an equal volume of 100 mM triethylammonium bicarbonate (TEAB) buffer, pH 8.5, containing 12 M urea. Dithiothreitol (DTT) was added from a 100 mM aqueous stock solution to a final concentration of 5 mM and the mixture incubated at 37 °C for 1 h. Then, iodoacetamide (or acrylamide) was added from a ca. 500 mM dimethyl sulfoxide (DMSO) stock solution to reach 50 mM and incubation at 37 °C was continued for another 30 min. Finally, the mixture was diluted 1:10 with 20% acetonitrile and 0.4% FA in water (to a DMSO concentration of 1%) and washed 6× with the same solvent in a 10 kDa cutoff centrifugal spin filter (Amicon Ultra Ultracel regenerated cellulose, Merck Millipore Ltd., Cork, Ireland), concentrated to ca. 100 μL, filtered through a 0.2 μm syringe filter (Minisart RC 4, Sartorius Stedim Lab Ltd., Stonehouse, UK), and injected by passing the LC into the QToF mass analyzer.

The viability of the method for quantitative determination of DF was demonstrated by analyzing a reference sample, consisting equal parts of Qβ[Hpg] (**1**) and Qβ[Sia1(100%)] (**5a**) as obtained by literature protocols.[25] The spectrum showed signals of equal intensity for both monomers (Figure S2).

Protein Concentration Determination. Concentrations of protein solutions were determined using a Pierce BCA Protein Assay Kit (ThermoFisher Scientific) according to the manufacturer's instructions. Absorption at 562 nm was measured on a Tecan Infinite M-Plex plate reader (Tecan Group Ltd., Männedorf, Switzerland) and results evaluated using the software Prism (version 5.04, GraphPad Software, Inc., San Diego, CA).

HAI Test. The hemagglutination assay was performed according to a standardized protocol.[4] EDTA-stabilized human donor blood (German Red Cross) was diluted with Dulbecco's phosphate-buffered saline (DPBS) and erythrocytes were pelleted at 1500 rcf, 10 min, 4 °C repeatedly until the supernatant remained clear. Erythrocytes were diluted with DPBS to obtain a suspension of a hematocrit of 1%, which was stored on ice. Concentrated virus stocks from −80 °C storage were thawed on ice. To determine viral activity, serial 1:2 dilutions in DPBS were prepared in a 96-well round bottom plate at a total volume of 25 μL after which 50 μL of 1% erythrocyte suspension was added to each well and the mixtures incubated for 1 h at r.t. Based on these results, a 4 HAU/5 μL virus suspension was prepared in DPBS. Accurate virus titer of this suspension was verified by another hemagglutination test starting from 4 HAU with 25 μL total volume in the first well.

For the HAI test, inhibitors were serially diluted in a 96-well round bottom plate at 20 μL total volume. Five microliters (4 HAU) of virus suspension was added and the mixtures incubated for 30 min at r.t. Ensuingly, 50 μL of 1% erythrocyte suspension was added to each well and the results documented following another hour of incubation. The endpoint of the inhibitor dilution series was the highest dilution to still cause complete inhibition of hemagglutination, which reflects the inhibitory constant K_i.[27−29]

K_i values for Qβ[Sia1] conjugates (**5a−e**) were measured in triplicates, K_i values for Qβ[Sia3] conjugates (**6a−f**), Qβ[Sia8] conjugates (**7a−g**), and those for conjugates with mixed linker lengths (**8** and **9**) were measured in duplicates, each during the course of one individual experiment (Table S1). The values depicted in Figures 1 and 3 are the arithmetic means of these replicates.

The values for DF = 50% shown in Figure 3 were obtained by interpolating the experimental data using a regression function of the type

$$K_i = 10^{a\cdot\log(\mathrm{DF}) + b} \quad (2)$$

where a is the slope of the graph and b is the ordinate intercept.

https://doi.org/10.1021/acs.bioconjchem.2c00166
Bioconjugate Chem. 2022, 33, 1269−1278

Cryoelectron Microscopy. To control the binding of the Qβ phage capsids to influenza virus by cryoTEM, Qβ-[Sia1(98%),TAMRA(2%)] (**9a**) (concentration 200 nmol/L) was incubated with 15 μL of IAV X31 (1.2 mg/mL total protein) with gentle agitation for 30 min at room temperature. A perforated (1 μm hole diameter) carbon film-covered microscopical 200 mesh grid (R1/4 batch of Quantifoil, MicroTools GmbH, Jena, Germany) was cleaned with chloroform and hydrophilized by 60 s glow discharging before a 5 μL aliquot of the sample solution was applied to the grid. The sample was vitrified by automatic blotting and plunge freezing with a FEI Vitrobot Mark IV (ThermoFisher Scientific Inc., Waltham, MA) using liquid ethane as the cryogen. The vitrified specimen was transferred to the autoloader of a FEI TALOS ARCTICA electron microscope (ThermoFisher Scientific Inc.) operated at an acceleration voltage of 200 kV. Micrographs were acquired on a FEI Falcon 3 direct electron detector (ThermoFisher Scientific Inc.) using a 100 μm objective aperture and a nominal magnification of 28,000× corresponding to a calibrated pixel size of 3.69 Å/pixel.

Dynamic Light Scattering. DLS was performed using a Zetasizer Nano-ZS instrument (Malvern Instruments, Malvern, UK).

Qβ-Sialoside Bioconjugation. For bioconjugation, Qβ-[Hpg] (**1**) was transferred from the NaN_3-containing storage buffer (100 mM potassium phosphate (KPi) + 0.02% NaN_3) to regular KPi using PD MidiTrap G-25 protein desalting columns (Cytivia, Marlborough, MA). Stock solutions of 100 mM Na ascorbate and 100 mM aminoguanidine·HCl in KPi buffer were prepared. Catalyst mix was prepared by mixing equal parts of 200 mM $Cu(OAc)_2$ and 1 M THPTA in water. In a snap cap reaction vial, 0.5−2 nmol Qβ[Hpg] (**1**) was mixed with 36,000 equiv aminoguanidine, 1800 equiv $Cu(OAc)_2$/9000 equiv THPTA from catalyst mix, and the indicated amounts of azide (see Table 1). If necessary, KPi was added to fill up the reaction vial. Finally, 36,000 equiv of Na-ascorbate was added and the capped vial incubated at 37 °C overnight.

Purification of the products was performed by 1−2 rounds of dialysis against KPi + 5 mM EDTA and one round of dialysis against KPi, followed by SEC. Products were stored at 4 °C in KPi + 0.02% NaN_3.

Theoretical Model for the Inhibitory Constant K_i. For an irregular arrangement of SA on the capsid, the distances d_1, d_2, and d_3 between the HA-binding pocket and the three closest SA groups differ from each other. We therefore determine the quadratic mean $\sqrt{(d_1^2 + d_2^2 + d_3^2)/3}$. We furthermore note that molecular dynamics simulation found $r_{ete} = r_0\sqrt{n}$ for the end-to-end distance of short PEG oligomers with r_0 = 5 Å and n being the polymerization index of the EG linker.[34] We use these results to calculate the weight when summing over all SA triplets and doublets.

To determine the effective number of matching SA triplets numerically, we consider a partially functionalized capsid, where the functionalized residues are chosen randomly. For each SA group, we determine two neighboring SA groups, such that the resulting SA triangle is closest to the triangular arrangement of the HA-binding pockets. Subsequently, the distances d_1, d_2, and d_3 are determined and the quadratic mean is calculated. To determine $N_{tri,eff}$ of the entire capsid, we sum over all SA triangles. Subsequently, the K_i of the capsid is averaged over 500 different random SA configurations for each DF. $N_{di,eff}$ is calculated in an analogous way.

A549 Infection with A/Panama. The evening before the infection, 8.000 cells/well are seeded into an Ibidi angioslide. The viruses are diluted in DMEM containing 1% penicillin/streptomycin (v/v), 1% L-glutamine (v/v), 0.2% BSA (w/v), and 2 μg/mL TPCK-trypsin to achieve an multiplicity of infection (MOI) of 11. The virus solution is incubated on ice for 30 min followed by 30 min of incubation at 37 °C.

Interaction of A/Panama with A549 Cells. A549 cells are incubated with Qβ[Sia1(98%),TAMRA(2%)] (**9a**) for 10 min on ice and washed off carefully. For the experiment in which A/Panama viruses are to be bound to the cell surface, cells are incubated with DID-labeled IAV (multiplicity of infection (MOI) 11) for 30 min on ice before 200 nM Qβ-[Sia1(98%),TAMRA(2%)] (**9a**) is added to the cells and incubated on ice for 10 min, then washed off carefully. DID-labeled IAV and Qβ[Sia1(98%),TAMRA(2%)] (**9a**) are mixed in a 1:1 (v:v) ratio and incubated for 30 min at room temperature. The mixture is provided to the A459 cells and incubated on ice for 10 min. Unbound complexes are carefully washed off. Live cell imaging was performed at 37 °C using a spinning disc confocal microscope.

Nucleoprotein (NP) Staining. For anti-NP AB staining, infected cells are fixed and permeabilized using 10% formalin with 0.2% Triton-X100 in PBS. Cells are blocked with PBS containing 2% BSA for 1 h at room temperature. The primary antibody is diluted 1:500 in BB and incubated for 1 h at 37 °C. After washing three times with PBS++, the secondary antibody is stained the same way.

■ ASSOCIATED CONTENT

Supporting Information

The Supporting Information is available free of charge at https://pubs.acs.org/doi/10.1021/acs.bioconjchem.2c00166.

Micrographs of the control experiment validating infection of A549 cells and analytical data (mass spectra and/or NMR spectra) for all synthesized compounds (PDF)

■ AUTHOR INFORMATION

Corresponding Authors

Andreas Herrmann − *Institut für Chemie und Biochemie, Freie Universität Berlin, 14195 Berlin, Germany*; Phone: +49 30 838 59385; Email: a.herrmann2@fu-berlin.de

Christian P. R. Hackenberger − *Leibniz-Forschungsinstitut für Molekulare Pharmakologie (FMP), 13125 Berlin, Germany; Institut für Chemie, Humboldt-Universität zu Berlin, 12489 Berlin, Germany*; orcid.org/0000-0001-7457-4742; Phone: +49-30-94793 181; Email: Hackenbe@fmp-berlin.de

Authors

Lutz Adam − *Leibniz-Forschungsinstitut für Molekulare Pharmakologie (FMP), 13125 Berlin, Germany; Institut für Chemie, Humboldt-Universität zu Berlin, 12489 Berlin, Germany*; orcid.org/0000-0003-3385-526X

Eva Müller − *Institut für translationale HIV Forschung, Universitätsklinikum Essen, 45147 Essen, Germany*

Kai Ludwig − *Forschungszentrum für Elektronenmikroskopie und Gerätezentrum BioSupraMol, Institut für Chemie und Biochemie, Freie Universität Berlin, Berlin 14195, Germany*

Simon Klenk − *Leibniz-Forschungsinstitut für Molekulare Pharmakologie (FMP), 13125 Berlin, Germany; Institut für*

Chemie, Humboldt-Universität zu Berlin, 12489 Berlin, Germany

Daniel Lauster − *Institut für Chemie und Biochemie, Freie Universität Berlin, 14195 Berlin, Germany*

Susanne Liese − *Max-Planck Institute for the Physics of Complex Systems, Dresden 01187, Germany; Institut für Physik, Universität Augsburg, Augsburg 86159, Germany*

Complete contact information is available at: https://pubs.acs.org/10.1021/acs.bioconjchem.2c00166

Notes

The authors declare no competing financial interest.

■ ACKNOWLEDGMENTS

The authors thank Andrew K. Udit for providing the Qβ(K16M) plasmid, as well as Saba Nojoumi and Kristin Kemitz-Hassanin for performing the bacterial expression of Qβ[Hpg] capsids. This work was supported by the German Research Foundation (DFG, SFB765, SPP1623, SFB1449—431232613) and the Berlin University Alliance (BUA; Corona Virus Pre-Exploration Project).

■ ABBREVIATIONS

cryoTEM: cryogenic transmission electron microscopy
CuAAC: Cu-catalyzed alkyne−azide cycloaddition
DF: degree of functionalization
DLS: dynamic light scattering
DMSO: dimethyl sulfoxide
DPBS: Dulbecco's phosphate-buffered saline
DTT: dithiothreitol
EG: ethylene glycol
HA: hemagglutinin
HAI: hemagglutination inhibition
Hpg: homopropargylglycine
IAV: influenza A virus
KPi: potassium phosphate
MOI: multiplicity of infection
NA: neuraminidase
Neu5Ac: *N*-acetylneuraminic acid
NP: (influenza) nucleoprotein
PDB: protein data bank
RBS: receptor binding site
SA: sialic acid
TAMRA: tetramethylrhodamine
TEAB: triethylammonium bicarbonate

■ REFERENCES

(1) Javanian, M.; Barary, M.; Ghebrehewet, S.; Koppolu, V.; Vasigala, V. K. R.; Ebrahimpour, S. A Brief Review of Influenza Virus Infection. *J. Med. Virol.* **2021**, *93*, 4638−4646.

(2) Lauster, D.; Glanz, M.; Bardua, M.; Ludwig, K.; Hellmund, M.; Hoffmann, U.; Hamann, A.; Böttcher, C.; Haag, R.; Hackenberger, C. P. R.; Herrmann, A. Multivalent Peptide − Nanoparticle Conjugates for Influenza-Virus Inhibition. *Angew. Chem., Int. Ed.* **2017**, *56*, 5931−5936.

(3) Kim, T. H.; Lee, S. W. Aptamers for Anti-Viral Therapeutics and Diagnostics. *Int. J. Mol. Sci.* **2021**, *22*, No. 4168.

(4) Bhatia, S.; Lauster, D.; Bardua, M.; Ludwig, K.; Angioletti-Uberti, S.; Popp, N.; Hoffmann, U.; Paulus, F.; Budt, M.; Stadtmüller, M.; et al. Linear Polysialoside Outperforms Dendritic Analogs for Inhibition of Influenza Virus Infection in Vitro and in Vivo. *Biomaterials* **2017**, *138*, 22−34.

(5) Makimura, Y.; Watanabe, S.; Suzuki, T.; Suzuki, Y.; Ishida, H.; Kiso, M.; Katayama, T.; Kumagai, H.; Yamamoto, K. Chemoenzymatic Synthesis and Application of a Sialoglycopolymer with a Chitosan Backbone as a Potent Inhibitor of Human Influenza Virus Hemagglutination. *Carbohydr. Res.* **2006**, *341*, 1803−1808.

(6) Ogata, M.; Murata, T.; Murakami, K.; Suzuki, T.; Hidari, K. I. P. J.; Suzuki, Y.; Usui, T. Chemoenzymatic Synthesis of Artificial Glycopolypeptides Containing Multivalent Sialyloligosaccharides with a γ-Polyglutamic Acid Backbone and Their Effect on Inhibition of Infection by Influenza Viruses. *Bioorg. Med. Chem.* **2007**, *15*, 1383−1393.

(7) Stadtmueller, M. N.; Bhatia, S.; Kiran, P.; Hilsch, M.; Reiter-Scherer, V.; Adam, L.; Parshad, B.; Budt, M.; Klenk, S.; Sellrie, K.; et al. Evaluation of Multivalent Sialylated Polyglycerols for Resistance Induction in and Broad Antiviral Activity against Influenza A Viruses. *J. Med. Chem.* **2021**, *64*, 12774−12789.

(8) Totani, K.; Kubota, T.; Kuroda, T.; Murata, T.; Hidari, K. I. P. J.; Suzuki, T.; Suzuki, Y.; Kobayashi, K.; Ashida, H.; Yamamoto, K.; et al. Chemoenzymatic Synthesis and Application of Glycopolymers Containing Multivalent Sialyloligosaccharides with a Poly(L-Glutamic Acid) Backbone for Inhibition of Infection by Influenza Viruses. *Glycobiology* **2003**, *13*, 315−326.

(9) Tsuchida, A.; Kobayashi, K.; Matsubara, N.; Muramatsu, T.; Suzuki, T.; Suzuki, Y. Simple Synthesis of Sialyllactose-Carrying Polystyrene and Its Binding with Influenza Virus. *Glycoconjugate J.* **1998**, *15*, 1047−1054.

(10) Papp, I.; Sieben, C.; Sisson, A. L.; Kostka, J.; Böttcher, C.; Ludwig, K.; Herrmann, A.; Haag, R. Inhibition of Influenza Virus Activity by Multivalent Glycoarchitectures with Matched Sizes. *ChemBioChem* **2011**, *12*, 887−895.

(11) Papp, I.; Sieben, C.; Ludwig, K.; Roskamp, M.; Böttcher, C.; Schlecht, S.; Herrmann, A.; Haag, R. Inhibition of Influenza Virus Infection by Multivalent Sialic-Acid- Functionalized Gold Nanoparticles. *Small* **2010**, *6*, 2900−2906.

(12) Meng, X.; Yang, M.; Li, Y.; Li, X.; Jia, T.; He, H.; Yu, Q.; Guo, N.; He, Y.; Yu, P.; Yang, Y. Multivalent Neuraminidase Hydrolysis Resistant Triazole-Sialoside Protein Conjugates as Influenza-Adsorbents. *Chin. Chem. Lett.* **2018**, *29*, 76−80.

(13) Artner, L. M.; Merkel, L.; Bohlke, N.; Beceren-Braun, F.; Weise, C.; Dernedde, J.; Budisa, N.; Hackenberger, C. P. R. Site-Selective Modification of Proteins for the Synthesis of Structurally Defined Multivalent Scaffolds. *Chem. Commun.* **2012**, *48*, 522−524.

(14) Mühlberg, M.; Hoesl, M. G.; Kuehne, C.; Dernedde, J.; Budisa, N.; Hackenberger, C. P. R. Orthogonal Dual-Modification of Proteins for the Engineering of Multivalent Protein Scaffolds. *Beilstein J. Org. Chem.* **2015**, *11*, 784−791.

(15) Bhatia, S.; Hilsch, M.; Cuellar-Camacho, J. L.; Ludwig, K.; Nie, C.; Parshad, B.; Wallert, M.; Block, S.; Lauster, D.; Böttcher, C.; et al. Adaptive Flexible Sialylated Nanogels as Highly Potent Influenza A Virus Inhibitors. *Angew. Chem., Int. Ed.* **2020**, *59*, 12417−12422.

(16) Nie, C.; Parshad, B.; Bhatia, S.; Cheng, C.; Stadtmüller, M.; Oehrl, A.; Kerkhoff, Y.; Wolff, T.; Haag, R. Topology-Matching Design of an Influenza-Neutralizing Spiky Nanoparticle-Based Inhibitor with a Dual Mode of Action. *Angew. Chem., Int. Ed.* **2020**, *59*, 15532−15536.

(17) Bhatia, S.; Donskyi, I. S.; Block, S.; Nie, C.; Burdinski, A.; Lauster, D.; Radnik, J.; Herrmann, A.; Haag, R.; Ludwig, K.; Adeli, M. Wrapping and Blocking of Influenza A Viruses by Sialylated 2D Nanoplatforms. *Adv. Mater. Interfaces* **2021**, *8*, No. 2100285.

(18) Nie, C.; Stadtmüller, M.; Parshad, B.; Wallert, M.; Ahmadi, V.; Kerkhoff, Y.; Bhatia, S.; Block, S.; Cheng, C.; Wolff, T.; Haag, R. Heteromultivalent Topology-Matched Nanostructures as Potent and Broad-Spectrum Influenza A Virus Inhibitors. *Sci. Adv.* **2021**, *7*, No. eabd3803.

(19) Guo, C. T.; Wong, C. H.; Kajimoto, T.; Miura, T.; Ida, Y.; Juneja, L. R.; Kim, M. J.; Masuda, H.; Suzuki, T.; Suzuki, Y. Synthetic Sialylphosphatidylethanolamine Derivatives Bind to Human Influenza A Viruses and Inhibit Viral Infection. *Glycoconjugate J.* **1998**, *15*, 1099−1108.

(20) Guo, C. T.; Sun, X. L.; Kanie, O.; Shortridge, K. F.; Suzuki, T.; Miyamoto, D.; Hidari, K. I. P. J.; Wong, C. H.; Suzuki, Y. An O-Glycoside of Sialic Acid Derivative That Inhibits Both Hemagglutinin

and Sialidase Activities of Influenza Viruses. *Glycobiology* **2002**, *12*, 183−190.
(21) Di Iorio, D.; Verheijden, M. L.; Van Der Vries, E.; Jonkheijm, P.; Huskens, J. Weak Multivalent Binding of Influenza Hemagglutinin Nanoparticles at a Sialoglycan-Functionalized Supported Lipid Bilayer. *ACS Nano* **2019**, *13*, 3413−3423.
(22) Waldmann, M.; Jirmann, R.; Hoelscher, K.; Wienke, M.; Niemeyer, F. C.; Rehders, D.; Meyer, B. A Nanomolar Multivalent Ligand as Entry Inhibitor of the Hemagglutinin of Avian Influenza. *J. Am. Chem. Soc.* **2014**, *136*, 783−788.
(23) Ohta, T.; Miura, N.; Fujitani, N.; Nakajima, F.; Niikura, K.; Sadamoto, R.; Guo, C.-T.; Suzuki, T.; Suzuki, Y.; Monde, K.; Nishimura, S. I. Glycotentacles: Synthesis of Cyclic Glycopeptides, Toward a Tailored Blocker of Influenza Virus Hemagglutinin. *Angew. Chem.* **2003**, *115*, 5344−5347.
(24) Bandlow, V.; Lauster, D.; Ludwig, K.; Hilsch, M.; Reiter-Scherer, V.; Rabe, J. P.; Böttcher, C.; Herrmann, A.; Seitz, O. Sialyl-LacNAc-PNA·DNA Concatamers by Rolling-Circle Amplification as Multivalent Inhibitors of Influenza A Virus Particles. *ChemBioChem* **2019**, *20*, 159−165.
(25) Lauster, D.; Klenk, S.; Ludwig, K.; Nojoumi, S.; Behren, S.; Adam, L.; Stadtmüller, M.; Saenger, S.; Zimmler, S.; Hönzke, K.; et al. Phage Capsid Nanoparticles with Defined Ligand Arrangement Block Influenza Virus Entry. *Nat. Nanotechnol.* **2020**, *15*, 373−379.
(26) Overeem, N. J.; van der Vries, E.; Huskens, J. A Dynamic, Supramolecular View on the Multivalent Interaction between Influenza Virus and Host Cell. *Small* **2021**, *17*, No. 2007214.
(27) Kaufmann, L.; Syedbasha, M.; Vogt, D.; Hollenstein, Y.; Hartmann, J.; Linnik, J. E.; Egli, A. An Optimized Hemagglutination Inhibition (HI) Assay to Quantify Influenzaspecific Antibody Titers. *J. Visualized Exp.* **2017**, *2017*, No. e55833.
(28) Pedersen, J. C. Hemagglutination-Inhibition Assay for Influenza Virus Subtype Identification and the Detection and Quantitation of Serum Antibodies to Influenza Virus. In *Animal Influenza Virus. Methods in Molecular Biology (Methods and Protocols)*; Spackman, E., Ed.; Humana Press: New York, NY, 2014; pp 11−25.
(29) Mammen, M.; Dahmann, G.; Whitesides, G. M. Effective Inhibitors of Hemagglutination by Influenza Virus Synthesized from Polymers Having Active Ester Groups. Insight into Mechanism of Inhibition. *J. Med. Chem.* **1995**, *38*, 4179−4190.
(30) Liese, S.; Netz, R. R. Quantitative Prediction of Multivalent Ligand-Receptor Binding Affinities for Influenza, Cholera, and Anthrax Inhibition. *ACS Nano* **2018**, *12*, 4140−4147.
(31) Golmohammadi, R.; Fridborg, K.; Bundule, M.; Valegård, K.; Liljas, L. The Crystal Structure of Bacteriophage Qβ at 3.5 Å Resolution. *Structure* **1996**, *4*, 543−554.
(32) Valegård, K.; Fridborg, K.; Liljas, L. Crystallization and Preliminary X-Ray Diffraction Studies of the Bacteriophage Qβ. *Acta Crystallogr., Sect. D: Biol. Crystallogr.* **1994**, *50*, 105−109.
(33) Haldar, J.; Álvarez De Cienfuegos, L.; Tumpey, T. M.; Gubareva, L. V.; Chen, J.; Klibanov, A. M. Bifunctional Polymeric Inhibitors of Human Influenza A Viruses. *Pharm. Res.* **2010**, *27*, 259−263.
(34) Liese, S.; Gensler, M.; Krysiak, S.; Schwarzl, R.; Achazi, A.; Paulus, B.; Hugel, T.; Rabe, J. P.; Netz, R. R. Hydration Effects Turn a Highly Stretched Polymer from an Entropic into an Energetic Spring. *ACS Nano* **2017**, *11*, 702−712.

https://doi.org/10.1021/acs.bioconjchem.2c00166
Bioconjugate Chem. 2022, 33, 1269−1278